

## Dendritic Iron(II) Porphyrins as Models for Hemoglobin and Myoglobin: Specific Stabilization of O<sub>2</sub> Complexes in Dendrimers with H-Bond-Donor Centers

by Adrien Zingg<sup>a)</sup>, Béatrice Felber<sup>a)</sup>, Volker Gramlich<sup>b)</sup>, Lei Fu<sup>c)</sup>, James P. Collman<sup>\*c)</sup>, and François Diederich<sup>\*a)</sup>

<sup>a)</sup> Laboratorium für Organische Chemie, ETH-Hönggerberg, HCI, CH-8093 Zürich

<sup>b)</sup> Laboratorium für Kristallographie, ETH-Zentrum, Sonneggstrasse 5, CH-8092 Zürich

<sup>c)</sup> Department of Chemistry, Stanford University, Stanford, CA 94305, U.S.A.

---

Two types of dendritically functionalized iron(II) porphyrins were prepared (*Scheme*) and investigated in the presence of 1,2-dimethylimidazole (1,2-DiMeIm) as the axial ligand as model systems for *T*(tense)-state hemoglobin (Hb) and myoglobin (Mb). Equilibrium O<sub>2</sub>- and CO-binding studies were performed in toluene and aqueous phosphate buffer (pH 7). UV/VIS Titrations (*Fig. 4*) revealed that the two dendritic receptors **1·Fe<sup>II</sup>-1,2-DiMeIm** and **2·Fe<sup>II</sup>-1,2-DiMeIm** (*Fig. 2*) with secondary amide moieties in the dendritic branching undergo reversible complexation (*Fig. 5*) with O<sub>2</sub> and CO in dry toluene. Whereas the CO affinity is similar to that measured for the natural receptors, the O<sub>2</sub> affinity is greatly enhanced and exceeds that of *T*-state Hb by a factor of *ca.* 1500 (*Table*). The oxygenated complexes possess half-lives of several h (*Fig. 6*). This remarkable stability originates from both dendritic encapsulation of the iron(II) porphyrin and formation of a H-bond between bound O<sub>2</sub> and a dendritic amide NH moiety (*Fig. 11*). Whereas reversible CO binding was also observed in aqueous solution (*Fig. 10*), the oxygenated iron(II) complexes are destabilized by the presence of H<sub>2</sub>O with respect to oxidative decay (*Fig. 9*), possibly as a result of the weakening of the O<sub>2</sub>···H–N H-bond by the competitive solvent. The comparison between the two dendrimers with amide branchings and ester derivative **3·Fe<sup>II</sup>-1,2-DiMeIm** (*Fig. 2*), which lacks H-bond donor centers in the periphery of the porphyrin, further supports the role of H-bonding in stabilizing the O<sub>2</sub> complex against irreversible oxidation. All three derivatives bind CO reversibly and with similar affinity (*Fig. 8*) in dry toluene, but the oxygenated complex of **3·Fe<sup>II</sup>-1,2-DiMeIm** undergoes much more rapid oxidative decomposition (*Fig. 7*).

---

**1. Introduction.** – Tetrameric hemoglobin (Hb) is an efficient transport protein for O<sub>2</sub> in aerobic organisms; its monomeric counterpart myoglobin (Mb) is responsible for O<sub>2</sub> storage in muscle tissues. The protein superstructure shields the iron(II) heme cofactor against irreversible oxidation and  $\mu$ -oxo dimer formation [1]. Furthermore, the peptidic shell plays an important role in tuning the affinity of the heme iron(II) [2][3] for diatomic gases (O<sub>2</sub>, CO, NO). In the deoxy forms of the two proteins, a ‘proximal’ imidazole from a His residue coordinates axially, leading to a five-coordinate high-spin Fe<sup>II</sup> center. Reversible O<sub>2</sub> binding occurs at the opposite porphyrin face, and a ‘distal’ imidazole from a second His residue is thought to interact with the terminal O-atom of the bound gas *via* H-bonding. This hypothesis was first proposed by *Pauling* in 1964 [4] and was later supported by neutron-diffraction data for oxymyoglobin [5] and oxyhemoglobin [6] (*Fig. 1*). The existence of such an H-bond was also demonstrated by electron paramagnetic resonance and resonance-*Raman* studies [7][8]. Although the strength of the H-bond between ‘distal’ imidazole and bound O<sub>2</sub> remains a matter of discussion [9], this interaction seems to play an important role in the discrimination of the heme proteins between O<sub>2</sub> and CO binding [10].

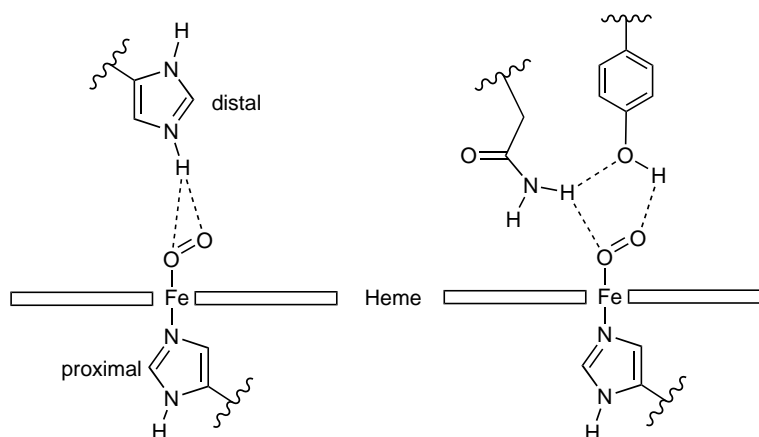


Fig. 1. H-Bonding in the O<sub>2</sub> complexes of vertebrate Hb and Mb [5][6] (left) and Hb of the bloodworm *Ascaris lumbricoides* (right) [26]

In Hb, the preference for CO over O<sub>2</sub> binding is around 200-fold and in Mb only 30-fold [11]; these values are critical for aerobic life [12]. In contrast, early synthetic iron(II) heme model systems [13][14], such as the ‘picket fence’ porphyrin [15–17], showed much higher affinities for CO over O<sub>2</sub>. The reduced CO affinity of Hb and Mb is assumed to result from steric [18–20] and/or a combination of polar and apolar interactions of the ligand with the surrounding protein [3][14e][21]. The ‘picket fence’ porphyrin was the first model system with an O<sub>2</sub> affinity about the same as that of *T*(tense)-state Hb. The polar binding pocket shaped by the four pivaloyl-amide residues kinetically stabilizes the intrinsically bent O<sub>2</sub> adduct, and a H-bond between one of the pivaloyl amide NH moieties and the coordinated O<sub>2</sub> was postulated [17]. More recent model systems with hindered binding cavities have been shown to complex O<sub>2</sub> with a slight preference over CO [22]. However, the detailed relationship between structural distortion from a linear CO-ligation geometry and equilibrium binding affinities remains controversial [3][13c][14c][23].

To investigate the influence of H-bonding on the O<sub>2</sub> affinity of Hb and Mb model systems, iron(II) porphyrin derivatives with and without H-bond donor functionality were prepared [14e][24]. Replacement of one of the four pivaloyl residues in the ‘picket fence’ iron(II) porphyrin by H-bond donor substituents was shown to reduce  $P_{1/2}(\text{O}_2)$  (the partial pressure of O<sub>2</sub> required to obtain half-saturation of the iron(II) heme coordination site) by a factor of 10 compared to the original receptor, *i.e.*, O<sub>2</sub> binding is strengthened. Protein engineering of Hb also underlines the critical role of the ‘distal’ imidazole residue for the fine-tuning of ligand affinity [25]. Further evidence for H-bonding stabilization of coordinated O<sub>2</sub> comes from the exceptionally high O<sub>2</sub> affinity of Hb of the bloodworm *Ascaris lumbricoides*. The X-ray crystal structure shows a network of H-bonds between coordinated O<sub>2</sub> and ‘distal’ tyrosine and glutamine residues (*Fig. 1*) [26]. Environmental polarity was also shown in model studies to slightly affect O<sub>2</sub> affinity [27].

Basic requirements for synthetic heme models are a five-coordinate iron(II) porphyrin in a high-spin state with a proximal N-base and a vacant coordination site for O<sub>2</sub>. To prevent formation of hemochromes by axial coordination of two N-bases to the iron(II) porphyrin (the equilibrium constant for the addition of the second ligand is higher than for the first one), different approaches have been adopted. Thus, addition of a sterically hindered axial base, such as 1,2-dimethylimidazole (1,2-DiMeIm) [28], favors formation of a five-coordinate high-spin complex with the Fe<sup>II</sup> center displaced out of the heme plane (a model for *T*-state Hb). Covalent attachment of the axial ligand to the heme [29] or steric hindrance of one of the two faces of the heme [30][31] are other approaches to prevent hemochrome formation. Rapid decomposition of the O<sub>2</sub> adducts *via*  $\mu$ -oxo-dimer formation is usually prevented by attachment of bulky substituents onto the iron(II) porphyrin as in the ‘picket fence’ systems [15] or by bridging the macrocycle [31][32]. Such protection can also be readily achieved by dendritic encapsulation as shown in this paper.

Over the past five years, the combination of metalloporphyrin with dendrimer chemistry [33] led to a fascinating new class of Hb and Mb model systems [34–36], with the dendritic superstructure mimicking the encapsulation of the heme in a natural protein environment [37]. Modification of the dendritic shell around the iron(II)-porphyrin core modulates the shape, density, and polarity of these model systems, thereby affecting profoundly thermodynamics and kinetics of complexes formed with O<sub>2</sub> and CO. Here, we report the gas-binding properties of two classes of water-soluble, dendritic iron(II) porphyrins, the first- and second-generation derivatives, **1**·Fe<sup>II</sup> and **2**·Fe<sup>II</sup>, respectively, with amide dendrons capable of H-bond donation, and first-generation compound **3**·Fe<sup>II</sup> with ester dendrons lacking H-bond donor centers in the dendritic shell (*Fig. 2*; for a preliminary communication of parts of this work, see [35]). UV/VIS Gas-binding titrations with O<sub>2</sub> and CO in different solvents in the presence of 1,2-DiMeIm reveal interesting effects of the chemical composition of the dendritic shell and environmental polarity on the stability of the formed complexes.

**2. Results.** – 2.1. *Synthesis of Dendritic Iron(II) Porphyrins.* The two target molecules **1**·Fe<sup>II</sup> and **2**·Fe<sup>II</sup> were obtained by a divergent strategy [38] as described in [39], whereas the convergent approach [40] was applied to the preparation of the novel first-generation dendrimer **3**·Fe<sup>II</sup> (*Scheme*).

The synthesis of the porphyrin core **4**·**2H** started from tetracarboxylic acid **5**·**Zn** [39c], which was reduced with BH<sub>3</sub>·THF to tetrol **4**·**Zn**. Crystals suitable for X-ray-analysis (*Fig. 3*) were obtained by vapor diffusion of cyclohexane into a solution of **4**·**Zn** in THF. The compound crystallized in the space group *C2/c* with two THF molecules axially coordinated to the Zn<sup>II</sup> center. The dihedral angle C(19)–C(20)–C(10)–C(9) between *meso*-phenyl ring and porphyrin nucleus amounts to 81.4°, orienting the four side chains into unhindered positions for attachment of the dendritic wedges. Demetallation of **4**·**Zn** with 0.4M HCl afforded **4**·**2H**, to which dendron **6** [41] was attached under *Mitsunobu* conditions [42] to give the dendritic porphyrin **3**·**2H**, which was purified by preparative gel permeation chromatography (GPC). The matrix-assisted laser-desorption-ionization time-of-flight (MALDI-TOF) mass spectrum (2-(4-hydroxyphenylazo)benzoic acid (HABA)) displayed the molecular ion as the parent ion at *m/z* 3547.1 (<sup>13</sup>C<sub>2</sub><sup>12</sup>C<sub>182</sub>H<sub>318</sub>N<sub>4</sub>O<sub>60</sub> requires

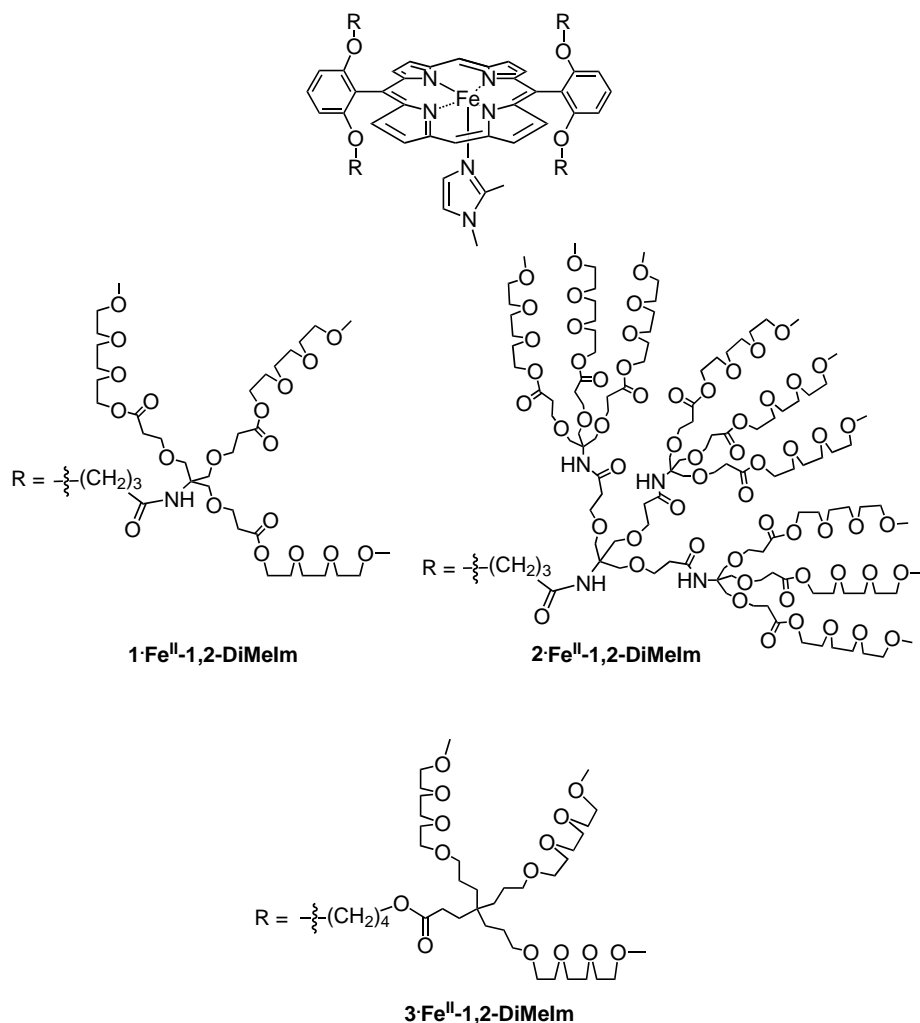
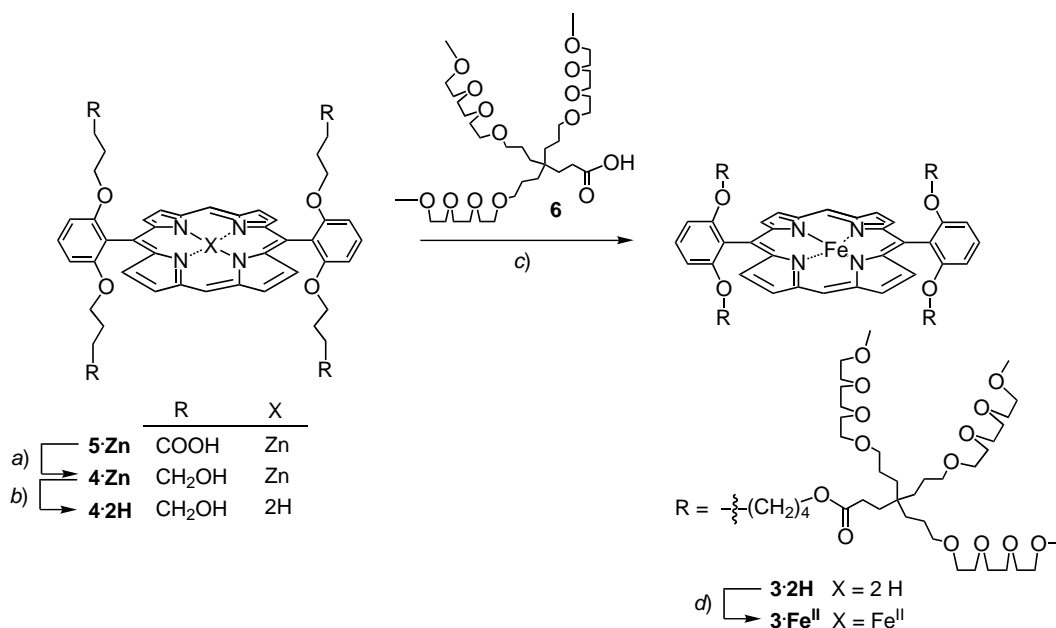


Fig. 2. Dendritic model compounds for T-state Hb

3546.2); no additional peaks resulting from fragmentation or impurities appeared in the spectrum. In the  $^{13}\text{C}$ -NMR spectrum (100 MHz,  $\text{CDCl}_3$ ) all twenty-eight resonances expected for **3·2H** were observed.

2.2. *Gas-Titration and -Binding Studies.* For the gas-binding studies, the  $\text{Fe}^{\text{II}}$  derivatives **1·Fe<sup>II</sup>**, **2·Fe<sup>II</sup>**, and **3·Fe<sup>II</sup>** were freshly prepared by metallation of the dendritic free-base porphyrins with  $\text{FeBr}_2$  in THF under inert atmosphere. UV/VIS Titrations were performed in a dry-box under  $\text{N}_2$  ( $[\text{O}_2] < 1$  ppm) according to a standard literature procedure and evaluated according to Eqn. 1 [22a] [43]

$$P(L) = \{[C_1]b\Delta\varepsilon\}P(L)/\Delta A - P_{1/2}(L) \quad (1)$$

Scheme. Synthesis of the Dendritic Fe<sup>II</sup> Porphyrin **3**·Fe<sup>II</sup>

a) BH<sub>3</sub>·THF, THF, r.t., 10 min, 65%. b) 0.4M aq. HCl, r.t., 2 h, then 1M aq. NaOH; 91%. c) Bu<sub>3</sub>P, THF, r.t., 5 min; then TMAD (N,N,N',N'-tetramethylazodicarboxamide), 80°, 1.5 h; 65%. d) FeBr<sub>2</sub>, 2,6-lutidine, THF, r.t., 1–4 h, 40–50%.

where  $P(L)$  [Torr] represents the partial pressure of the added gas L inside a tonometer,  $P_{1/2}(L)$  [Torr] the partial pressure of L at half-saturation binding to the Fe<sup>II</sup> porphyrin, and  $\Delta A$  the difference in optical absorbance of the solution of the Fe<sup>II</sup> porphyrin at  $P(L)$  and in the absence of L. The term  $\{[C_1]b\Delta\epsilon\}$  is a constant under the conditions of the measurements.

The total concentration of the Fe<sup>II</sup> porphyrin was kept constant during one titration. Its solution was prepared under N<sub>2</sub> and added to the tonometer, followed by *ca.* 20 equiv. of 1,2-DiMeIm to selectively form the five-coordinate high-spin complex [28]. Known amounts of O<sub>2</sub> or CO (L) were added *via* gas syringe into the septum-capped tonometer. After each addition, UV/VIS spectra were recorded. Plots of  $P(L)$  as a function of  $P(L)/\Delta A$  according to *Eqn. 1* provided a straight line, and from the intersect with the ordinate, the value of  $P_{1/2}(L)$  (equal to  $1/K_L$ , the reciprocal of the equilibrium formation constant of the 1:1 complex) was obtained. To maintain a constant pressure inside the tonometer during the entire titration, before each addition of L, the same amount of gas mixture was first removed. The partial pressure of L inside the tonometer at titration point  $n$ ,  $P_n$  [Torr] was subsequently calculated according to *Eqn. 2*

$$P_n = [P_{n-1}(V - v) + 760v]/V \quad (2)$$

where  $P_{n-1}$  is the partial pressure of L at titration point  $n - 1$ ,  $V$  the total volume in the tonometer not filled by the solution of the Fe<sup>II</sup> porphyrin, and  $v$  the volume of added L

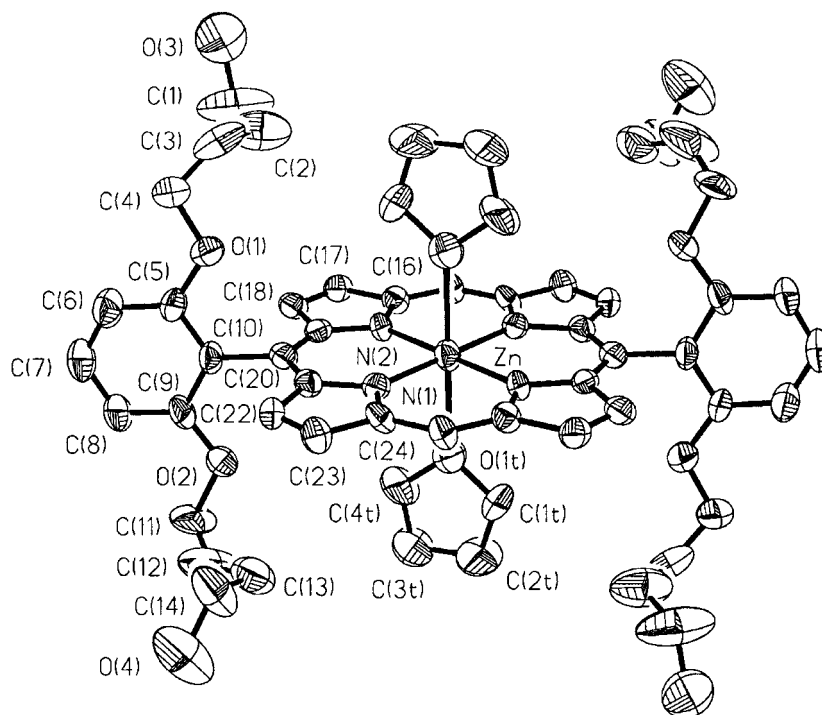


Fig. 3. ORTEP Plot of  $4 \cdot \text{Zn}$ . Arbitrary numbering. Atomic displacement parameters obtained at 293 K are shown at the 30% probability level. For clarity, the cyclohexane solvate inclusions are omitted.

(identical to the volume of gas mixture removed from the tonometer before addition of L). UV/VIS Spectra at each titration point were recorded after equilibration, which was indicated by constant absorbance of the solution in the tonometer.

A representative evaluation of experimental titration data (298 K), which were obtained in triplicate runs in each case, is given in Fig. 4 for the determination of  $P_{1/2}(\text{O}_2)$  ( $=0.016$  Torr) for the second-generation dendrimer  $2 \cdot \text{Fe}^{\text{II}}\text{-1,2-DiMeIm}$  in dry toluene. The Table shows the  $\text{O}_2$  and CO affinities of the two dendritic  $\text{Fe}^{\text{II}}$  porphyrins compared with those of human T-state Hb and Mb, T-state 'picket fence'  $\text{Fe}^{\text{II}}$  porphyrin, and Hb from the bloodworm *Ascaris lumbricoides*. Such comparison of data from different solvents should consider that environmental polarity may slightly affect the gas-binding affinity [27]. It is readily apparent that the two dendritic receptors display exceptionally high  $\text{O}_2$  affinities.

**2.2.1. Binding of  $\text{O}_2$  and CO to the Dendritic  $\text{Fe}^{\text{II}}$  Porphyrins  $1 \cdot \text{Fe}^{\text{II}}\text{-1,2-DiMeIm}$  and  $2 \cdot \text{Fe}^{\text{II}}\text{-1,2-DiMeIm}$  in Dry Toluene.** Binding of  $\text{O}_2$  to the dendritic  $\text{Fe}^{\text{II}}$  receptors in dry toluene is reversible. Upon exposure of a solution of  $1 \cdot \text{Fe}^{\text{II}}\text{-1,2-DiMeIm}$  ( $c \approx 3 \cdot 10^{-6}$  M) to  $\text{O}_2$ , the Soret band ( $\lambda_{\text{max}}$  427 nm) of the five-coordinate species vanished while a new, hypsochromically shifted maximum ( $\lambda_{\text{max}}$  421 nm), indicative of the six-coordinate  $\text{O}_2$  complex, appeared (Fig. 5). After deoxygenation and introduction of  $\text{N}_2$  by three 'freeze-pump' cycles, the spectrum of the original five-coordinate complex  $1 \cdot \text{Fe}^{\text{II}}\text{-1,2-DiMeIm}$  with the Soret band at 427 nm was fully recovered. This process was repeated

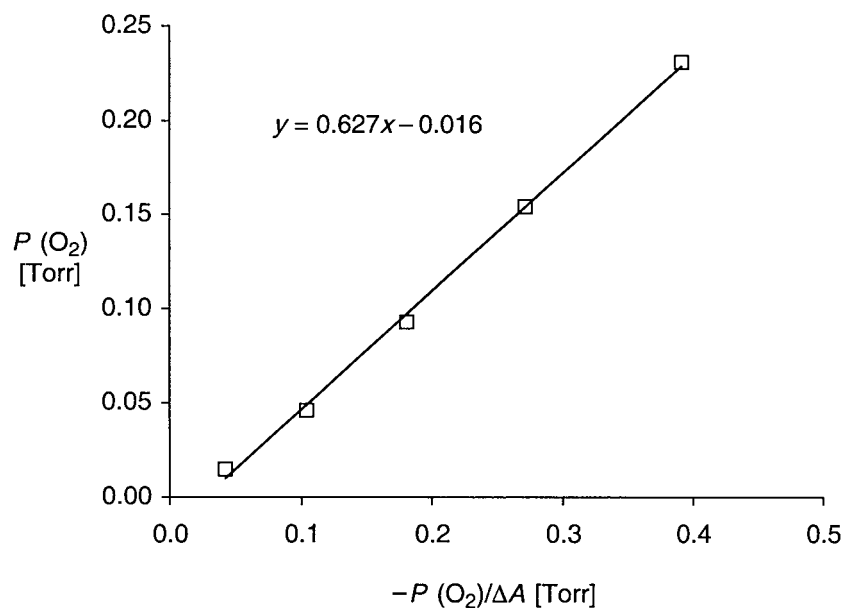


Fig. 4. UV/VIS Titration to determine the  $\text{O}_2$  affinity of **2**· $\text{Fe}^{\text{II}}$ -**1,2-DiMeIm** in dry toluene at 298 K. [**2**· $\text{Fe}^{\text{II}}$ ] ca.  $3 \cdot 10^{-6}$  M; [**1,2-DiMeIm**] ca.  $3-4 \cdot 10^{-5}$  M.  $P(\text{O}_2)$  = partial pressure of  $\text{O}_2$  in the tonometer,  $\Delta A$  = change in optical absorbance measured at 421 nm.

Table.  $\text{O}_2$  and CO Affinities of Dendritic  $\text{Fe}^{\text{II}}$  Porphyrins Determined by UV/VIS Titrations (298 K). Also shown are the gas-binding affinities of human T-state Hb and Mb [15][16b][44], T-state  $\text{Fe}^{\text{II}}$  'picket fence' porphyrin [15][16], and Hb from the bloodworm *Ascaris lumbricoides* [45]. The  $M$  value is the ratio of the two equilibrium binding constants  $K_{\text{CO}}/K_{\text{O}_2}$ , where  $K_{\text{CO}} = 1/P_{1/2}(\text{CO})$  and  $K_{\text{O}_2} = 1/P_{1/2}(\text{O}_2)$ , and denotes the selectivity of the heme  $\text{Fe}^{\text{II}}$  for  $\text{O}_2$  relative to CO<sup>a</sup>).

Porphyrin	$P_{1/2}(\text{O}_2)$ [Torr]	$P_{1/2}(\text{CO})$ [Torr]	$M$
T-State Hb <sup>b</sup> )	40	0.3	135
Mb <sup>b</sup> )	0.37–1	0.014–0.025	20–40
T-State iron(II) 'picket fence' porphyrin <sup>c</sup> )	38	0.0089	4280
<i>Ascaris lumbricoides</i> <sup>b</sup> )	0.002	0.1	0.02
<b>1</b> · $\text{Fe}^{\text{II}}$ - <b>1,2-DiMeIm</b> <sup>d</sup> )	0.035	0.35	0.1
<b>2</b> · $\text{Fe}^{\text{II}}$ - <b>1,2-DiMeIm</b> <sup>d</sup> )	0.016	0.19	0.08
<b>3</b> · $\text{Fe}^{\text{II}}$ - <b>1,2-DiMeIm</b> <sup>d</sup> )	– <sup>e</sup> )	0.075	
<b>1</b> · $\text{Fe}^{\text{II}}$ - <b>1,2-DiMeIm</b>	– <sup>e</sup> ) <sup>f</sup> )	0.052 <sup>b</sup> )	
<b>2</b> · $\text{Fe}^{\text{II}}$ - <b>1,2-DiMeIm</b>	– <sup>e</sup> ) <sup>f</sup> )	0.066 <sup>b</sup> )	
<b>3</b> · $\text{Fe}^{\text{II}}$ - <b>1,2-DiMeIm</b>	– <sup>e</sup> ) <sup>f</sup> )	– <sup>e</sup> ) <sup>b</sup> )	

<sup>a</sup>) Gas solubilities [ $\text{mol}^{-1} \text{atm}^{-1}$ ] in  $\text{H}_2\text{O}$ :  $1.157 \cdot 10^{-3}$  ( $\text{O}_2$ ),  $8.49 \cdot 10^{-4}$  (CO); in toluene:  $5.3 \cdot 10^{-3}$  ( $\text{O}_2$ ),  $7.39 \cdot 10^{-3}$  (CO) [46]. <sup>b</sup>) In aqueous phosphate buffer ( $\text{NaH}_2\text{PO}_4/\text{Na}_2\text{HPO}_4$ , pH 7), 293 K. <sup>c</sup>) In toluene in the presence of **1,2-DiMeIm**, 298 K. <sup>d</sup>) In dry toluene. <sup>e</sup>) Rapid irreversible oxidation prevented the determination of the stability of the oxygenated  $\text{Fe}^{\text{II}}$  complex by UV/VIS titrations. <sup>f</sup>) In  $\text{H}_2\text{O}$ -saturated toluene.

several times, indicating substantial stability of the  $\text{O}_2$  complex. After the reversibility was established, the binding affinity was quantitatively assessed in UV/VIS titrations as described above.

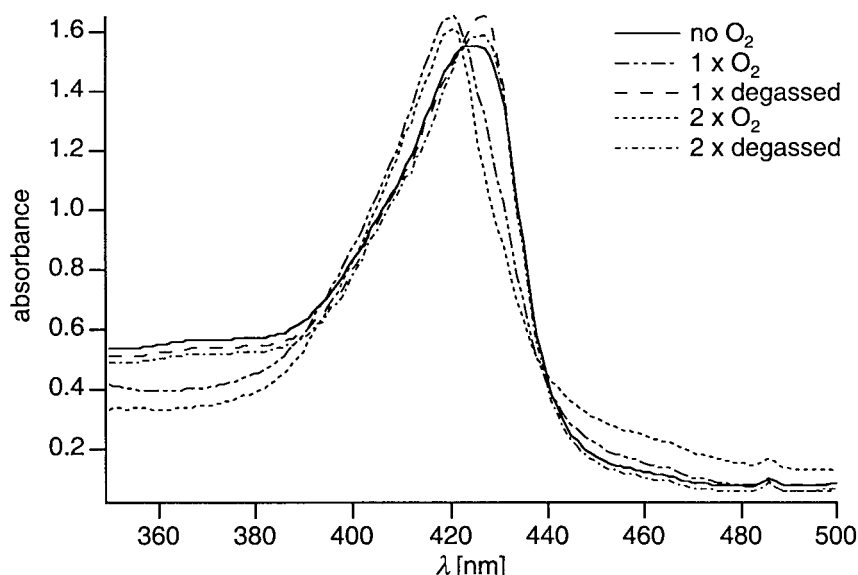


Fig. 5. Reversibility of  $O_2$  binding by  $1 \cdot Fe^{II}\text{-}1,2\text{-DiMeIm}$  in dry toluene at 298 K studied by UV/VIS spectroscopy.  $[1 \cdot Fe^{II}]$  ca.  $3 \cdot 10^{-6}$  M;  $[1,2\text{-DiMeIm}]$  ca.  $3\text{--}4 \cdot 10^{-5}$  M. Each state was kept for 30 min.

The stability of  $O_2$ -bound  $1 \cdot Fe^{II}\text{-}1,2\text{-DiMeIm}$  in dry toluene with respect to irreversible oxidative decomposition was investigated. For this purpose, a solution of the dendrimer in dry toluene was exposed to dry  $O_2$  in a septum-sealed UV cuvette, and the changes in the UV/VIS spectrum were recorded in 30-min intervals over a period of 3 d at 298 K (Fig. 6). The oxygenated  $Fe^{II}$  porphyrin underwent slow irreversible oxidation to an  $Fe^{III}$  complex, as indicated by the appearance of a new, hypsochromically shifted, broad Soret band at ca. 406 nm. The nature of this species was not investigated; a literature survey revealed that the mechanism for degradation of oxygenated  $Fe^{II}$  porphyrins in aprotic environments is not well-understood [1a][14b][24a]. Fitting of the experimental data to a first-order exponential decay provided  $k \approx 3.8 \cdot 10^{-5} \text{ s}^{-1}$  and a half-life  $t_{1/2}$  of ca. 5 h.

The reversibility of CO-binding to  $1 \cdot Fe^{II}\text{-}1,2\text{-DiMeIm}$  was also clearly demonstrated by UV/VIS spectroscopy. Here again, the maximum of the Soret band shifted reversibly from 427 nm in the initial five-coordinate complex to 421 nm in the six-coordinate CO complex, and the initial spectrum was fully recoverable after several 'CO then  $N_2$ ' gas flow cycles.

**2.2.2. Binding of  $O_2$  and CO to the Dendritic  $Fe^{II}$  Porphyrin  $3 \cdot Fe^{II}\text{-}1,2\text{-DiMeIm}$  in Dry Toluene.** The gas-binding behavior of this dendrimer differs substantially from that measured for the corresponding first-generation dendrimer  $1 \cdot Fe^{II}\text{-}1,2\text{-DiMeIm}$ . Upon addition of  $O_2$  in dry toluene at 298 K, the Soret band of the five-coordinate species at ca. 430 nm was rapidly replaced by a new absorption at 414 nm, characteristic of the oxygenated six-coordinate species [47][48]. However, the lifetime of this complex was too short to determine its stability by UV/VIS titrations. The intensity of the band at 414 nm rapidly decreased with concomitant appearance of a new broad Soret band at



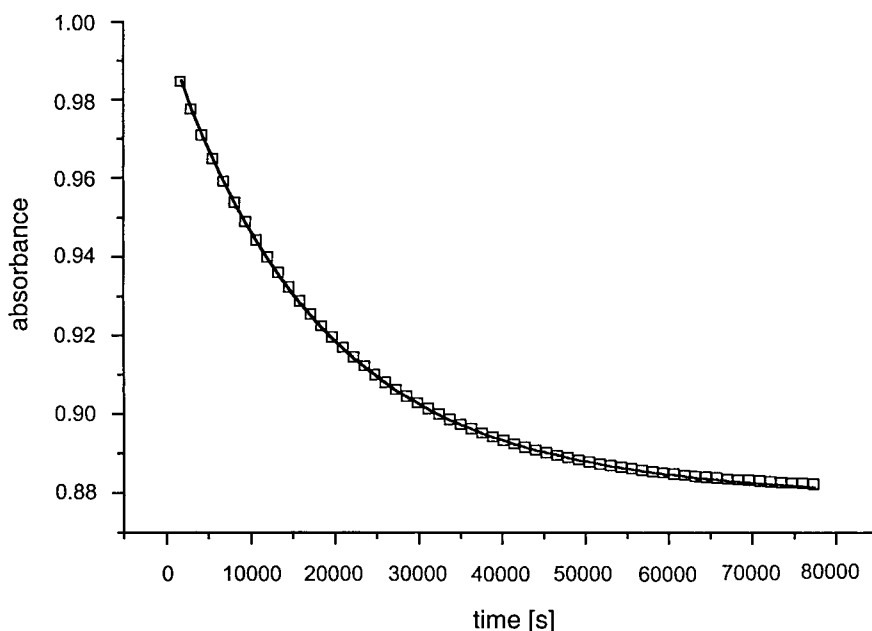


Fig. 6. Decomposition of oxygenated **1·Fe<sup>II</sup>-1,2-DiMeIm** in dry toluene at 298 K monitored by UV/VIS spectroscopy (421 nm). [**1·Fe<sup>II</sup>**] *ca.*  $3 \cdot 10^{-6}$  M; [**1,2-DiMeIm**] *ca.*  $3-4 \cdot 10^{-5}$  M. Spectra were taken at intervals of 30 min.

406 nm, corresponding to an irreversibly oxidized Fe<sup>III</sup> species (Fig. 7). The decrease in absorbance during the first 3 h was fitted to a first-order exponential decay, yielding  $k \approx 3 \cdot 10^{-4} \text{ s}^{-1}$  and  $t_{1/2} \approx 30$  min.

In contrast, CO forms a stable complex with **3·Fe<sup>II</sup>-1,2-DiMeIm** and the binding affinity ( $P_{1/2}(\text{CO}) = 0.075$  Torr) was found *ca.* 3–4 times higher than that measured for the two amide dendrimers (Table). Complexation is reversible and the five-coordinate (Soret band at 430 nm) and six-coordinate (Soret band at 414 nm) complexes could be fully interconverted in several ‘CO then N<sub>2</sub>’ gas flow cycles. Fig. 8 shows that the initial spectrum of **3·Fe<sup>II</sup>-1,2-DiMeIm** in deoxygenated, dry toluene depicts a mixture of both five-coordinate (430 nm) and six-coordinate (414 nm) species. The latter presumably results from coordination of minimal traces of residual O<sub>2</sub> (residual O<sub>2</sub> content in the dry-box *ca.* 0.5–1 ppm) or possibly solvent (THF) tenaciously entrapped in the dendritic shell. Gratifyingly, however, when O<sub>2</sub> after the first oxygenation was replaced again by N<sub>2</sub>, the absorption at 414 nm disappeared, leaving a clean solution of the five-coordinate species (Fig. 8).

Formation of clean solutions of five-coordinate Fe<sup>II</sup> porphyrin was actually problematic with all three dendrimers. However, by simply heating the solution to 50°, the Soret band for the six-coordinate species always disappeared, leaving only the band at *ca.* 430 nm corresponding to the five-coordinate complex. Upon cooling back to 298 K, the two bands were usually recovered with initial relative intensities. This process could be repeated many times, establishing the reversibility of this weak initial sixth ligation.

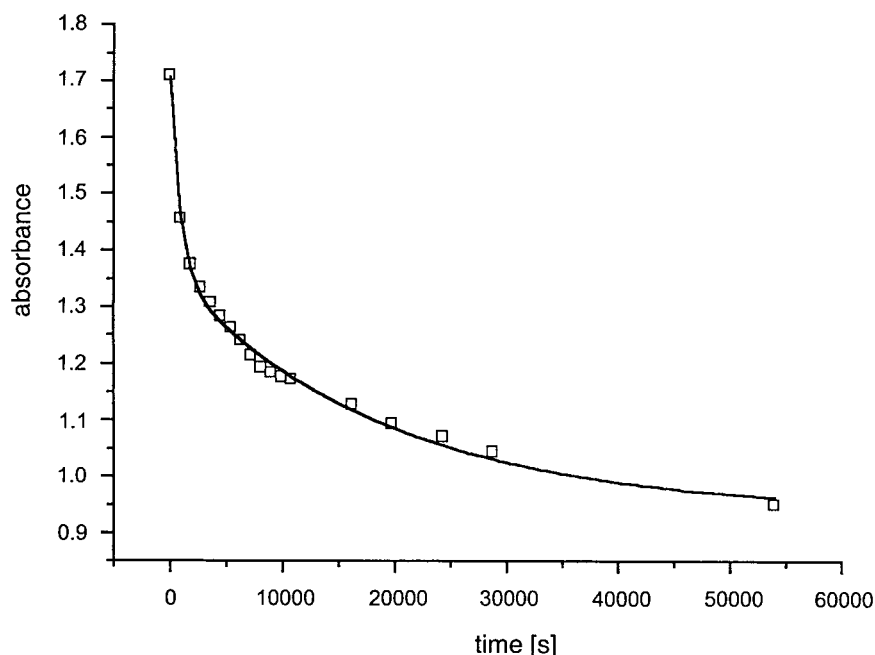


Fig. 7. Decomposition of oxygenated  $3 \cdot \text{Fe}^{\text{II}}\text{-1,2-DiMeIm}$  in dry toluene at 298 K monitored by UV/VIS spectroscopy (414 nm).  $[\mathbf{3} \cdot \text{Fe}^{\text{II}}]$  ca.  $4 \cdot 10^{-6}$  M;  $[\mathbf{1,2-DiMeIm}]$  ca.  $3\text{--}4 \cdot 10^{-5}$  M. Spectra were taken at intervals of 30 min.

**2.2.3. Binding of  $\text{O}_2$  and CO by the Three Dendritic  $\text{Fe}^{\text{II}}$  Porphyrins in Aqueous Solution.** In preliminary studies, we investigated  $\text{O}_2$  binding by  $\mathbf{1} \cdot \text{Fe}^{\text{II}}\text{-1,2-DiMeIm}$  and  $\mathbf{2} \cdot \text{Fe}^{\text{II}}\text{-1,2-DiMeIm}$  in water-saturated toluene. In contrast to the findings in dry toluene, the association of  $\text{O}_2$  could no longer be evaluated by UV/VIS titrations, since irreversible oxidation to  $\text{Fe}^{\text{III}}$  species, characterized by a broad *Soret* band at 406 nm, took place rather rapidly. With the first-generation compound, this irreversible oxidation was so fast that it could not be followed by our techniques. With the second-generation dendrimer, the oxidation was slow enough to be monitored by UV/VIS spectroscopy (Fig. 9). The decrease in the absorbance at 421 nm (six-coordinate  $\text{O}_2$  complex) was recorded at 15-min intervals and the experimental data fitted to a pseudo-first-order exponential decay yielding  $k \approx 1.3 \cdot 10^{-4} \text{ s}^{-1}$  and a half-life  $t_{1/2} \approx 2 \text{ h}$ .

With their triethyleneglycol monomethyl ether surface groups, the dendritic  $\text{Fe}^{\text{II}}$  porphyrins are readily soluble in aqueous phosphate buffer at pH 7 and CO binding by  $\mathbf{1} \cdot \text{Fe}^{\text{II}}\text{-1,2-DiMeIm}$  and  $\mathbf{2} \cdot \text{Fe}^{\text{II}}\text{-1,2-DiMeIm}$  was investigated in this biologically more relevant environment. Complexation was found to be reversible, and the CO affinities ( $P_{1/2}(\text{CO})$ , Table) were determined by UV/VIS titrations, monitoring the disappearance of the *Soret* band for the initial five-coordinate complex at 430 nm and the appearance of the band at 416 nm, characteristic for the six-coordinate CO complex (Fig. 10). Both dendrimers display similar affinity for CO (first generation:  $P_{1/2}(\text{CO}) = 0.052 \text{ Torr}$ ; second generation:  $P_{1/2}(\text{CO}) = 0.066 \text{ Torr}$ ), showing very little effect of

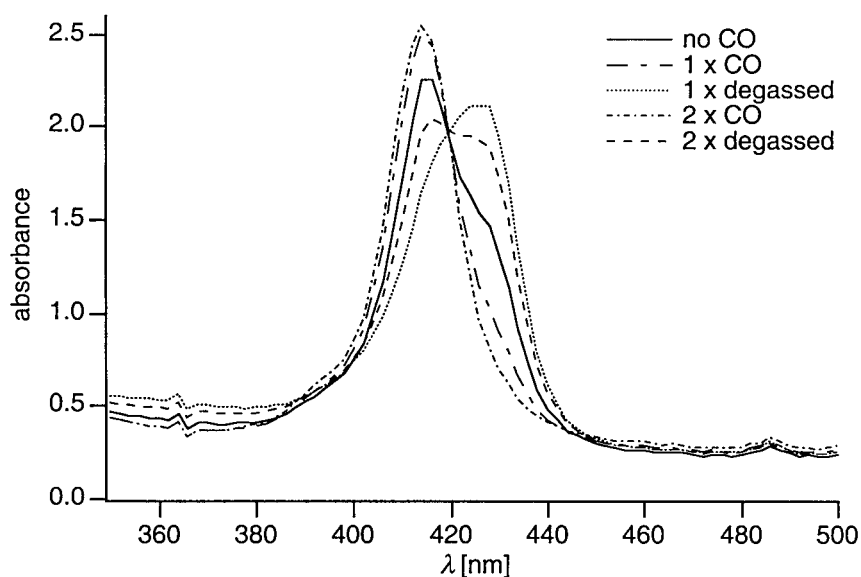


Fig. 8. Reversibility of CO binding by  $3 \cdot \text{Fe}^{\text{II}}\text{-1,2-DiMeIm}$  in dry toluene at 298 K studied by UV/VIS spectroscopy.  $[\mathbf{3} \cdot \text{Fe}^{\text{II}}]$  ca.  $3 \cdot 10^{-6}$  M;  $[\mathbf{1,2-DiMeIm}]$  ca.  $3\text{--}4 \cdot 10^{-5}$  M. Each state was kept for 30 min.

dendritic size. In several ‘CO to N<sub>2</sub>’ gas-flow cycles, the reversibility of CO binding was ascertained. Quantitative O<sub>2</sub>-binding studies were not conducted in aqueous buffer due to rapid irreversible oxidation of the oxygenated Fe<sup>II</sup> porphyrins.

Ester dendrimer  $3 \cdot \text{Fe}^{\text{II}}\text{-1,2-DiMeIm}$  was also found to decompose rapidly in aqueous environment, and quantitative gas-binding studies could not be performed. The origin of this decomposition, which occurred even in the absence of O<sub>2</sub> and led to the appearance of the broad Soret band at 406 nm, which is characteristic of Fe<sup>III</sup> species, was not further investigated.

**3. Discussion.** – The two dendrimer-based T-state hemoglobin models  $1 \cdot \text{Fe}^{\text{II}}\text{-1,2-DiMeIm}$  and  $2 \cdot \text{Fe}^{\text{II}}\text{-1,2-DiMeIm}$  of first and second generation, respectively, show reversible O<sub>2</sub> and CO binding in dry toluene (Table and Figs. 4 and 5). It is remarkable that their O<sub>2</sub> affinities ( $K_{\text{O}_2} = 1/P_{1/2}(\text{O}_2)$ ) are ca. 1500 times higher than those of T-state Hb and ca. 10–30 times higher than those of Mb [44]. In fact, these values approach the high O<sub>2</sub> affinity of Hb from the bloodworm *Ascaris lumbricoides* [26][45]. On the other hand, both dendrimers show a relatively low CO affinity, within the same range as T-state Hb and Mb. The combination of high O<sub>2</sub> and low CO affinities yields very low values for  $M$ , the ratio of the two equilibrium binding constants  $K_{\text{CO}}/K_{\text{O}_2}$ , where  $K_{\text{CO}} = 1/P_{1/2}(\text{CO})$  and  $K_{\text{O}_2} = 1/P_{1/2}(\text{O}_2)$ . Thus, the selectivity of the dendritic systems for binding O<sub>2</sub> over CO is similar to that seen for Hb from *Ascaris lumbricoides*. Interestingly, both CO- and O<sub>2</sub>-binding affinities are not much dependent of the degree of dendritic generation.

Why are the O<sub>2</sub> affinities so high? These may result from the formation of a H-bond between the bound gas and one of the NH residues of the amide moieties linking

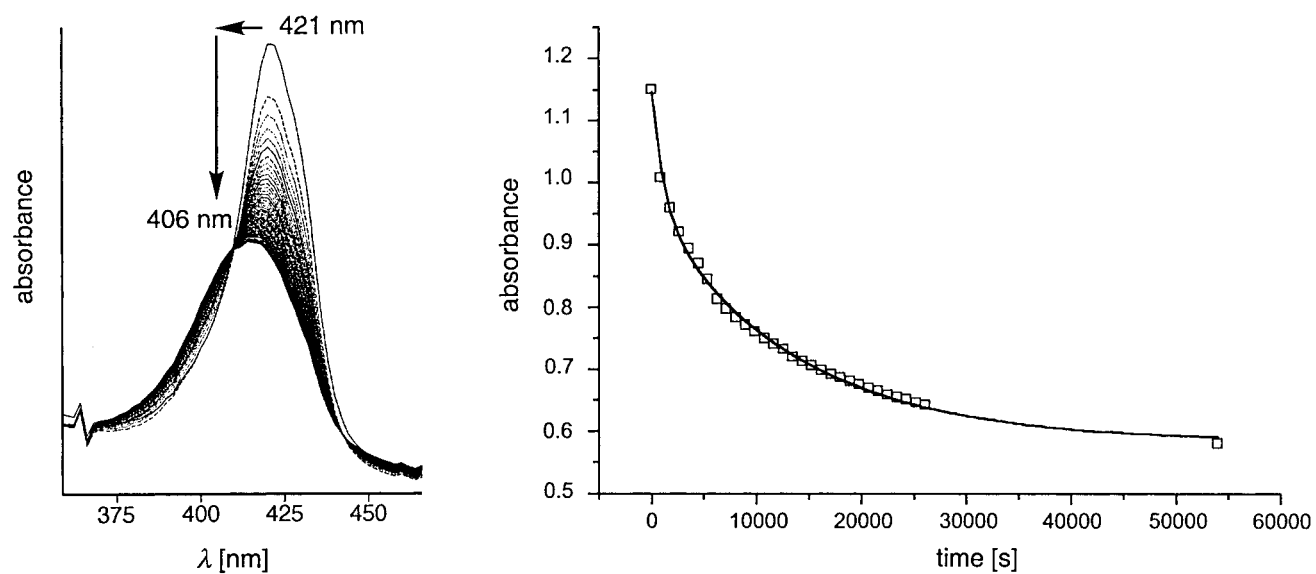


Fig. 9. Decomposition of oxygenated  $2 \cdot \text{Fe}^{\text{II}}\text{-1,2-DiMeIm}$  in aqueous toluene at 298 K monitored by UV/VIS spectroscopy.  $[\text{2} \cdot \text{Fe}^{\text{II}}]$  ca.  $3 \cdot 10^{-6}$  M;  $[1,2\text{-DiMeIm}]$  ca.  $3\text{--}4 \cdot 10^{-5}$  M. Spectra were recorded at intervals of 15 min. *Left*: disappearance of the *Soret* band of the oxygenated  $\text{Fe}^{\text{II}}$  complex at 421 nm and appearance of a broad, new *Soret* band at ca. 406 nm originating from irreversible oxidation to an  $\text{Fe}^{\text{III}}$  complex of unknown structure. *Right*: decrease of the absorbance at 421 nm as a function of time.

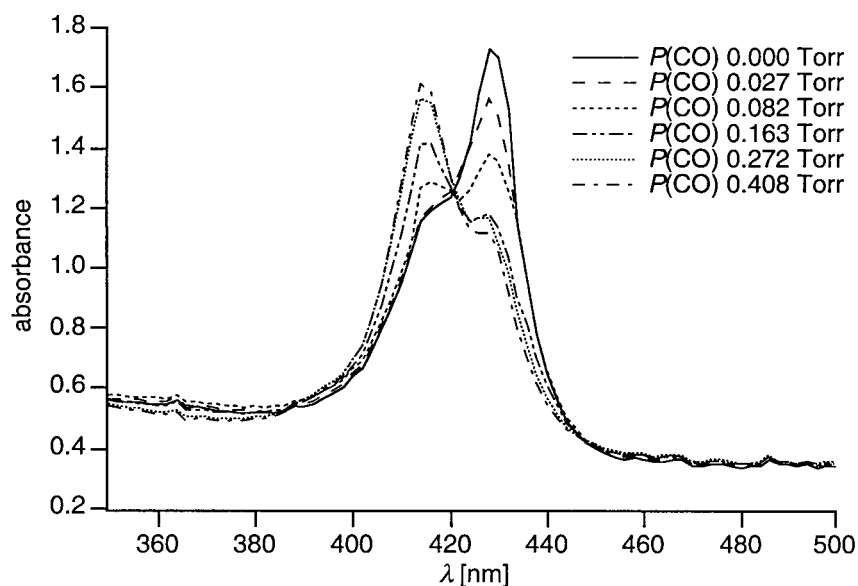


Fig. 10. UV/VIS Titration to determine the CO affinity of  $2 \cdot \text{Fe}^{\text{II}}\text{-1,2-DiMeIm}$  in aqueous phosphate buffer (pH 7) at 298 K.  $[\text{2} \cdot \text{Fe}^{\text{II}}]$  ca.  $3 \cdot 10^{-6}$  M;  $[\text{1,2-DiMeIm}]$  ca.  $3\text{--}4 \cdot 10^{-5}$  M.

together the porphyrin core and the first-generation dendritic branches. Such H-bonding, schematically shown in Fig. 11, is supported by computer-model examinations. The lower CO affinities may be caused by a congested pocket over the CO-binding site. A reduction of CO affinities in more hindered binding cavities and, as a consequence, a lowering of  $M$ , in some cases even below 1 [22b], has been observed with other model systems, such as ‘pocket’, ‘hybrid’, and ‘capped’ porphyrins [18–20]. However, as mentioned in the *Introduction*, the relationship between structural distortion and equilibrium binding affinities of CO remains controversial.

Whereas  $\text{O}_2$  complexes of simple  $\text{Fe}^{\text{II}}$  porphyrins decompose rapidly [1], the dendritic shell provides substantial stabilization against irreversible oxidation to  $\text{Fe}^{\text{III}}$  complexes, as has been previously observed [34][36]. Thus, the oxidative decay of the  $\text{O}_2$  complexes formed in dry toluene occurs only over the course of several hours (Fig. 6). Expectedly, the first-generation derivative, with a less encapsulated heme nucleus, decomposes much more rapidly (as shown by the studies in  $\text{H}_2\text{O}$ -saturated toluene; Sect. 2.2.3, Fig. 9). It should be noted that the  $\text{Fe}^{\text{II}}$  hemes in Hb and Mb are also continuously oxidized to  $\text{Fe}^{\text{III}}$  species. Thus,  $t_{1/2}$  of oxygenated beef-heart Mb is 3.3 d at pH 9, 11 h at pH 7, and only 30 min at pH 5 [1c], and similar half-lives are measured for oxygenated human Hb ( $t_{1/2} = 7$  h at pH 7) [1d].

The stability of the oxygenated dendritic  $\text{Fe}^{\text{II}}$  porphyrin depends on solvent polarity. In dry toluene, the  $\text{O}_2$  complex of the first-generation derivative  $1 \cdot \text{Fe}^{\text{II}}\text{-1,2-DiMeIm}$  has a half-life  $t_{1/2} \approx 5$  h (Fig. 6), whereas, in  $\text{H}_2\text{O}$ -saturated toluene, the first-generation complex decomposes rapidly, and the second-generation complex has a half-life  $t_{1/2} \approx 2$  h (Fig. 9). This facile irreversible oxidation to  $\text{Fe}^{\text{III}}$  species prevented the determination of  $\text{O}_2$  affinities in  $\text{H}_2\text{O}$ -saturated toluene. We considered these findings a

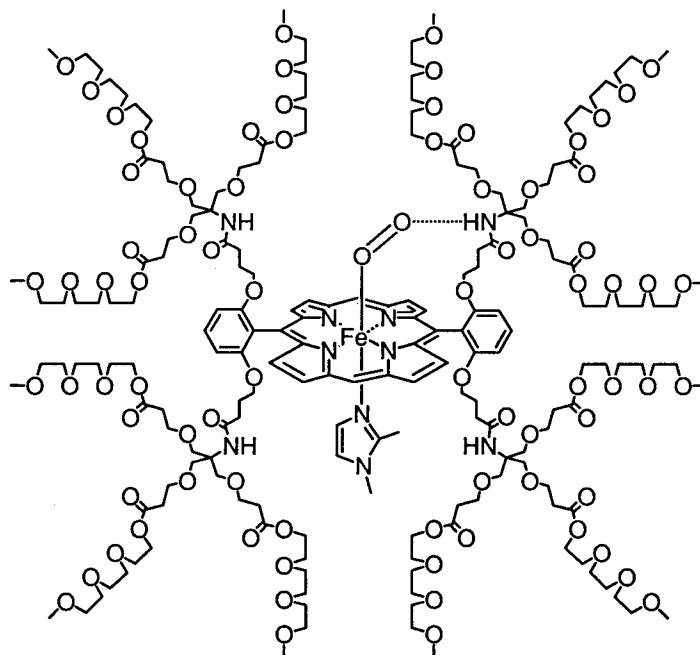


Fig. 11. Schematic representation of the postulated H-bond stabilizing the  $O_2$  complex of  $1 \cdot Fe^{II}\text{-}1,2\text{-DiMeIm}$

first indication for a dual role of the proposed  $O_2 \cdots H-N$  H-bond in the dendritic complexes (Fig. 11). It not only enhances the  $O_2$  affinity by shifting the equilibrium between five- and six-coordinate  $Fe^{II}$  species, but also slows down irreversible oxidation processes under formation of  $Fe^{III}$  species. In dry toluene, the H-bond is strong, whereas, in aqueous solutions, it is weakened by competition from the solvent.

The CO affinities of the two dendritic iron porphyrins are 3–6 times higher in  $H_2O$  than in dry toluene. Differences in the hydrodynamic volume [49][50] of the dendrimers could contribute to these changes in affinity. In  $H_2O$ , favorable interactions between the dendritic oligoether branches and the solvent induce a larger hydrodynamic volume, whereas, in dry toluene, the polar branches presumably pack tightly together in order to avoid contact with the apolar solvent. As a consequence, steric distortion of CO binding is increased in toluene, resulting in a reduced association strength.

To further investigate the possible role of H-bonding in  $O_2$  and CO binding by  $1 \cdot Fe^{II}\text{-}1,2\text{-DiMeIm}$  and  $2 \cdot Fe^{II}\text{-}1,2\text{-DiMeIm}$ , we prepared the first-generation dendrimer  $3 \cdot Fe^{II}\text{-}1,2\text{-DiMeIm}$  lacking any H-bond donor functionality in the dendritic side chains. The gas-binding behavior of this new derivative differed greatly. In dry toluene, reversible CO complexation was observed and UV/VIS titrations (Fig. 10) revealed that ligation strength was *ca.* 4.5 times higher than in the complex of  $1 \cdot Fe^{II}\text{-}1,2\text{-DiMeIm}$ . Binding of  $O_2$  to  $3 \cdot Fe^{II}\text{-}1,2\text{-DiMeIm}$  was also indicated by a shift of the *Soret* band from 430 nm (five-coordinate complex) to 414 nm (six-coordinate complex). However, irreversible oxidation to  $Fe^{III}$  species was too rapid to allow quantitative

determination of O<sub>2</sub> affinity by UV/VIS titration. With  $t_{1/2} \approx 30$  min, the half-lifetime of the oxygenated Fe<sup>II</sup> complex is much shorter than that of the corresponding complex formed by **1·Fe<sup>II</sup>-1,2-DiMeIm** ( $t_{1/2} \approx 5$  h).

In aqueous solutions, the stability of the O<sub>2</sub> complex of **3·Fe<sup>II</sup>-1,2-DiMeIm** was not only further reduced, but the dendrimer was found to decompose rapidly even in the absence of O<sub>2</sub>, thereby preventing any quantitative gas-binding studies. The decomposed dendrimer showed a broad *Soret* band at *ca.* 406 nm, indicative for formation of Fe<sup>III</sup> species which were not further investigated.

The comparison between the gas-binding affinities of the two first-generation compounds **1·Fe<sup>II</sup>-1,2-DiMeIm** and **3·Fe<sup>II</sup>-1,2-DiMeIm** in dry toluene provides important support for the proposed role of H-bonding in O<sub>2</sub> complexation. Both derivatives undergo reversible CO binding with similar ligation strength; clearly H-bonding is not much altering the CO affinity. On the other hand, the O<sub>2</sub> complex of **3·Fe<sup>II</sup>-1,2-DiMeIm**, which is not stabilized by H-bonding, decomposes much more readily than the complex of **1·Fe<sup>II</sup>-1,2-DiMeIm**, for which the O<sub>2</sub>···H–N H-bond is postulated. Further investigations are now underway to provide additional support for the important hypothesis raised in this study that the host-guest H-bond in O<sub>2</sub> complexes of the natural receptors Hb and Mb, and synthetic model systems not only enhances the binding affinity but additionally stabilizes the oxygenated complex against irreversible oxidative decomposition.

**4. Conclusion.** – Three dendritic Fe<sup>II</sup> porphyrins were prepared and investigated as models for *T*-state Hb and Mb. UV/VIS Titrations revealed that the two receptors **1·Fe<sup>II</sup>-1,2-DiMeIm** and **2·Fe<sup>II</sup>-1,2-DiMeIm** containing secondary-amide groups in the dendritic branching undergo stable, reversible complexation with O<sub>2</sub> and CO in dry toluene, with the O<sub>2</sub> affinity greatly surpassing that of *T*-state Hb (by a factor of *ca.* 1500) or Mb (by a factor of *ca.* 10–30). The oxygenated complexes are stable for several hours due to the protection against  $\mu$ -oxo dimer formation provided by the dendritic shell. The enhanced stability of the O<sub>2</sub> complexes and their reduced propensity to undergo irreversible oxidation to Fe<sup>III</sup> species are presumably also a result of the formation of a H-bond between bound O<sub>2</sub> and amide NH groups in the dendritic branches. CO Affinities in dry toluene were reduced by the same magnitude as those measured for the natural proteins, which was tentatively explained by steric distortion resulting from the dendritic shell. Reversible CO binding was also observed in aqueous phosphate buffer, whereas the oxygenated Fe<sup>II</sup> complexes are less stable in the presence of H<sub>2</sub>O. This reduced stability is presumably a result from the weakening of the intermolecular O<sub>2</sub>···H–N H-bond by the competitive solvent. Further support for the importance of this H-bond was obtained in the studies of dendrimer **3·Fe<sup>II</sup>-1,2-DiMeIm** that lacks H-bond-donor centers in its dendritic shell. Whereas this receptor undergoes reversible stable CO binding in dry toluene, the oxygenated complexes are unstable and undergo facile oxidative decomposition. Studies are now in progress to further clarify the proposed dual role of the H-bond in both stabilizing the O<sub>2</sub> complexes of Fe<sup>II</sup> porphyrins in natural and synthetic receptors and preventing their oxidative decomposition.

We thank the ETH research council, the *US National Science Foundation*, and *F. Hoffmann-La Roche*, Basel, for their support of this work.

### Experimental Part

*General.* Commercial chemicals and solvents were used without further purification unless otherwise stated. THF and toluene were freshly distilled from sodium benzophenone ketyl,  $\text{CH}_2\text{Cl}_2$  from  $\text{CaH}_2$ . Solvents used in an inert-gas atmosphere (dry-box;  $[\text{O}_2]: < 1 \text{ ppm}$ ), were deoxygenated by three ‘freeze-pump’ cycles. The aq. phosphate buffer (pH 7) was obtained by dissolving a mixture of  $\text{NaH}_2\text{PO}_4$  and  $\text{Na}_2\text{HPO}_4$  until a stable pH was reached. Evaporation in *vacuo* was conducted at  $\text{H}_2\text{O}$ -aspirator pressure. Products were dried at 0.05 Torr before anal. characterization. Column chromatography (CC):  $\text{SiO}_2$  60 (230–400 mesh, 0.040–0.063 mm) from *Fluka* or *Merck*. M.p.: *Büchi B-540*; uncorrected. Prep. gel-permeation chromatography (GPC): glass column (140 × 4 cm) filled with *Bio-Rad Bio-Beads® S-X1* (200–400 mesh); elution with  $\text{CH}_2\text{Cl}_2$ . IR spectra [ $\text{cm}^{-1}$ ]: *Perkin-Elmer 1600-FT IR*.  $^1\text{H}$ - and  $^{13}\text{C}$ -NMR spectra: *Bruker AMX-400* and *Varian Gemini 200*; spectra were recorded at 298 K with solvent peak as reference. MS ( $m/z$  (%)): FAB: *VG ZAB2-SEQ* spectrometer with 3-nitrobenzyl alcohol (NOBA) as matrix; MALDI-TOF: *Bruker-Reflex* spectrometer with HABA as matrix. Elemental analyses were performed by the Mikrolabor at the Laboratorium für Organische Chemie, ETH-Zürich.

*Determination of the Gas-Binding Constants.*  $\text{O}_2$  and  $\text{CO}$  affinities were determined by UV/VIS titrations at 298 K according to the procedure in [22a][43] with a *Hewlett-Packard 8452A* diode-array spectrophotometer.  $\text{O}_2$  (2.58% in  $\text{N}_2$ ) and  $\text{CO}$  (99.95%) were used from *Matheson Gas Products*. Receptor solns. were prepared under  $\text{N}_2$  by mixing the  $\text{Fe}^{\text{II}}$  porphyrins ( $c = 3 - 5 \cdot 10^{-6} \text{ M}$ ) with a *ca.* 20-fold amount of 1,2-DiMeIm in a dry-box ( $[\text{O}_2] < 1 \text{ ppm}$ ) to selectively form the five-coordinate complexes [28][47]. The solns were put into a tonometer of defined volume, which was sealed with a septum. Gases were added with a special gas-titration syringe. Partial gas pressures at each titration point were calculated according to *Eqn. 2* and binding affinities ( $P_{1/2} [\text{Torr}] = 1/K_1$ ) were determined according to *Eqn. 1*.

*Determination of First-Order Rate Constants for Oxidative Decomposition of Oxygenated Iron(II) Porphyrins.* In a dry-box at 298 K, a soln. of  $\text{Fe}^{\text{II}}$  porphyrin (*ca.*  $3 \cdot 10^{-6} \text{ M}$ ) and 1,2-DiMeIm (*ca.*  $3 - 4 \cdot 10^{-5} \text{ M}$ ) in dry or aq. toluene was put into a UV-cuvette sealed with a septum. *Via* a gas syringe, 5 ml of  $\text{O}_2$  were bubbled through the soln. to form the  $\text{O}_2$  complex, and UV/VIS spectral changes (at 421 nm for oxygenated **1-Fe<sup>II</sup>-1,2-DiMeIm** in dry toluene and oxygenated **2-Fe<sup>II</sup>-1,2-DiMeIm** in aq. toluene, and at 414 nm for oxygenated **3-Fe<sup>II</sup>-1,2-DiMeIm** in dry toluene) were recorded at 15–30 min intervals with the diode-array spectrophotometer over a period of 15 h to 3 d. The decrease in absorbance as a function of time was fitted to a first-order exponential decay.

*General Procedure for Fe<sup>II</sup>-Ion Insertion into the Free-Base Porphyrins.* A soln. of the free-base porphyrin (*ca.* 1–2 mg; *ca.* 0.004–0.008 mmol),  $\text{Fe}^{\text{II}}\text{Br}_2$  (*Aldrich, puriss. p.a.*; 6 mg, 0.03 mmol), and 2,6-lutidine (1 drop) in THF (3 ml) was stirred in a dry-box at r.t. for 1–4 h. The solvent was evaporated, and toluene was added. The reddish suspension was filtered through *Celite* to remove any inorg. residue. The solvent was again evaporated, and the resulting red oil was purified by CC (small  $\text{SiO}_2$  column, THF as eluent, single red band), providing the  $\text{Fe}^{\text{II}}$  porphyrin in *ca.* 40–50% yield.

*X-Ray Crystal Structure of 4·Zn.* Crystal data at 293 K for  $\text{C}_{48}\text{H}_{52}\text{N}_4\text{O}_8\text{Zn} \cdot 2 \text{C}_4\text{H}_8\text{O} \cdot 2 \text{C}_6\text{H}_{12}$  ( $M_r$  1190.89): monoclinic, space group  $C2/c$ ,  $D_c = 1.352 \text{ g cm}^{-3}$ ,  $Z = 4$ ,  $a = 26.38(3)$ ,  $b = 13.003(10)$ ,  $c = 18.86(2) \text{ \AA}$ ,  $\beta = 106.51(10)^\circ$ ,  $V = 6203(11) \text{ \AA}^3$ . *Picker-Stoe* diffractometer,  $\text{CuK}_\alpha$  radiation,  $\lambda = 1.54178 \text{ \AA}$ . The structure was solved by direct methods (SHELXTL PLUS) and refined with 377 parameters by full-matrix least-squares analysis based on  $F^2$  using experimental weights; all heavy atoms were refined anisotropically, H-atoms fixed isotropically with positions calculated from stereochemical considerations. Final  $R(F) = 0.1011$  for 3174 observed reflections with  $I > 2\sigma(I)$  and  $wR(F^2) = 0.2396$  for all 3174 data. *Cambridge Crystallographic Data Centre* deposition No. CCDC-165189. Copies of the crystallographic data (excluding structure factors) can be obtained, free of charge, on application to the *Cambridge Crystallographic Data Centre*, 12 Union Road, Cambridge CB21EZ, UK (fax: +44(1223)336033; e-mail: deposit@ccdc.cam.ac.uk).

(*SP-4-I*)-[[4,4',4'',4'''-*2IH,23H-Porphine-5,15-diylbis[benzene-2,1,3-triylldioxy]]tetrakisbutan-1-olo]](2-)- $\text{N}^{21},\text{N}^{22},\text{N}^{23},\text{N}^{24}$ ]zinc (**4·Zn**). To **5·Zn** (15 mg, 0.016 mmol) in THF (2 ml),  $\text{BH}_3 \cdot \text{THF}$  (1M, 0.5 ml, 0.5 mmol) was added, and the soln. was stirred at r.t. After 10 min, MeOH (2 ml) was added, and the mixture was dried ( $\text{Na}_2\text{SO}_4$ ). CC ( $\text{SiO}_2$ ;  $\text{CH}_2\text{Cl}_2/\text{MeOH}$  1:1) and recrystallization (THF/cyclohexane) provided **4·Zn** (61 mg, 65%). Fine purple crystals. M.p. 293°. IR (KBr): 3411, 2922, 2866, 1577, 1455, 1388, 1246, 1098, 1055, 991, 838,*



777, 716. UV/VIS (CHCl<sub>3</sub>): 311 (11200), 352 (6300), 395 (26900), 415 (323600), 511 (1500), 547 (11000), 582 (2000), 616 (700). <sup>1</sup>H-NMR (200 MHz, (CD<sub>3</sub>)<sub>2</sub>SO): 0.65–0.79 (*m*, 8 H), 0.99–1.13 (*m*, 8 H); 2.83–2.91 (*m*, 8 H); 3.93 (*t*, *J* = 6.4, 8 H); 7.27 (*d*, *J* = 8.3, 4 H); 7.87 (*t*, *J* = 8.3, 2 H); 8.93 (*d*, *J* = 4.3, 4 H); 9.45 (*d*, *J* = 4.3, 4 H); 10.27 (*s*, 2 H). <sup>13</sup>C-NMR (50 MHz, (CD<sub>3</sub>)<sub>2</sub>SO): 29.8; 32.9; 64.6; 72.7; 109.6; 110.4; 116.4; 125.8; 134.9; 136.2 (2 ×); 153.4; 154.7; 164.5. FAB-MS: 876.4 (100, *MH*<sup>+</sup>). Anal. calc. for C<sub>48</sub>H<sub>52</sub>N<sub>4</sub>O<sub>8</sub>Zn · 2.5H<sub>2</sub>O (923.35): C 62.44, H 6.22, N 6.07; found: C 62.42, H 5.95, N 6.16. *X-Ray* Analysis: see Fig. 3.

4,4',4'',4'''-[21H,23H-Porphine-5,15-diylbis[benzene-2,1,3-triylldioxy]]tetrakis(butane-1-ol) (**4·2H**). To **4·2H** (148 mg, 0.17 mmol) in CH<sub>2</sub>Cl<sub>2</sub> (20 ml), 0.4M HCl (5 ml, 2 mmol) was added, and the mixture was stirred at r.t. for 2 h. The deep red soln. turned green. After addition of 1M NaOH, the phases were separated, and the aq. phase was extracted with CHCl<sub>3</sub>. The combined org. phases were dried (Na<sub>2</sub>SO<sub>4</sub>) and evaporated. CC (SiO<sub>2</sub>; CH<sub>2</sub>Cl<sub>2</sub>/MeOH 93:7) and recrystallization (THF) gave **4·2H** (124 mg, 91%). Fine, deep-purple needles. M.p. 298°. IR (KBr): 3388, 3288, 3133, 2933, 2866, 1583, 1455, 1405, 1250, 1100, 955, 838, 783, 766, 738, 711. UV (CHCl<sub>3</sub>): 391 (60200), 408 (275400), 504 (15100), 538 (4500), 574 (5200), 642 (1200). <sup>1</sup>H-NMR (200 MHz, (CD<sub>3</sub>)<sub>2</sub>SO): –3.14 (*s*, 2 H); 0.63–0.76 (*m*, 8 H); 0.99–1.14 (*m*, 8 H); 2.85 (*t*, *J* = 5.9, 8 H); 4.04 (*t*, *J* = 6.6, 8 H); 7.31 (*d*, *J* = 8.4, 4 H); 7.43 (*br. s*, 4 H); 7.92 (*t*, *J* = 8.4, 2 H); 9.03 (*d*, *J* = 4.8, 4 H); 9.63 (*d*, *J* = 4.8, 4 H); 10.6 (*s*, 2 H). <sup>13</sup>C-NMR (50 MHz, (CD<sub>3</sub>)<sub>2</sub>SO): 29.8, 32.9, 64.5, 72.8, 109.4, 110.4, 116.4, 123.2, 135.3, 135.8, 136.7, 149.5, 151.9, 164.3. FAB-MS: 815.3 (100, *M*<sup>+</sup>). HR-FAB-MS: 815.4022 (*M*<sup>+</sup>, C<sub>48</sub>H<sub>54</sub>N<sub>4</sub>O<sub>8</sub>; calc. 814.9787).

[21H,23H-Porphine-5,15-diylbis[benzene-2,1,3-triylldioxy]]tetrakis(butane-1,4-diyl)tetrakis[7-[2-[2-(2-methoxyethoxy)ethoxy]ethoxy]-4,4-bis(3-[2-[2-(2-methoxyethoxy)ethoxy]ethoxy]propyl)heptanoate] (**3·2H**). To a degassed soln. of **4·2H** (5 mg, 0.00614 mmol) and **6** (50 mg, 0.0713 mmol) in abs. THF (2 ml), Bu<sub>3</sub>P (*ca.* 85%; 20 ml, 0.0713 mmol) was added, and the mixture was stirred at r.t. for 5 min. After addition of TMAD (13 mg, 0.0713 mmol), the mixture was heated for 1.5 h to 80°. Evaporation and CC (SiO<sub>2</sub>; CH<sub>2</sub>Cl<sub>2</sub>/MeOH 93:7), followed by prep. GPC (*Bio-Beads S-X1*; CH<sub>2</sub>Cl<sub>2</sub>) gave **3·2H** (14.2 mg, 65%). Deep-red viscous oil. IR (CHCl<sub>3</sub>): 3011, 1516, 1422, 1211, 1138, 927, 755, 672. UV (CHCl<sub>3</sub>): 409 (338800), 503 (16200), 536 (5000), 576 (5700), 631 (1700), 645 (1600). <sup>1</sup>H-NMR (400 MHz, CDCl<sub>3</sub>): –3.06 (*s*, 2 H); 0.73 (*q*, *J* = 6.8, 8 H); 1.02–1.13 (*m*, 32 H); 1.34–1.48 (*m*, 32 H); 1.96–2.02 (*m*, 8 H); 3.34–3.61 (*m*, 212 H); 3.89 (*t*, *J* = 5.8, 8 H); 7.03 (*d*, *J* = 8.5, 4 H); 7.73 (*t*, *J* = 8.5, 2 H); 8.96 (*d*, *J* = 4.5, 4 H); 9.28 (*d*, *J* = 4.5, 4 H); 10.16 (*s*, 2 H). <sup>13</sup>C-NMR (100 MHz, CDCl<sub>3</sub>): 23.3, 24.2, 24.8, 28.4, 31.0, 32.2, 36.3, 59.0, 63.2, 67.4, 70.0, 70.1, 70.5, 70.6, 71.8, 71.9, 72.0, 104.1, 105.3, 111.3, 119.6, 130.3, 130.4, 131.0, 144.9, 147.5, 159.8, 173.8. MALDI-TOF-MS: 3547.1 (100, *M*<sup>+</sup>; calc. for [<sup>12</sup>C<sub>182</sub><sup>13</sup>C<sub>2</sub>H<sub>318</sub>N<sub>4</sub>O<sub>60</sub>]<sup>+</sup>; 3546.2). Anal. calc. for C<sub>184</sub>H<sub>318</sub>N<sub>4</sub>O<sub>60</sub> (3546.53): C 62.32, H 9.04, N 1.58; found: C 62.07, H 9.08, N 1.68.

## REFERENCES

- [1] a) K. Shikama, *Chem. Rev.* **1998**, *98*, 1357; b) M. Tsuruga, K. Shikama, *Biochim. Biophys. Acta* **1997**, *1337*, 96; c) Y. Sugawara, K. Shikama, *Eur. J. Biochem.* **1980**, *110*, 241; d) A. Mansouri, K. H. Winterhalter, *Biochem.* **1973**, *12*, 4946.
- [2] M. F. Perutz, *Ann. Rev. Biochem.* **1979**, *48*, 327.
- [3] B. A. Springer, S. G. Sligar, J. S. Olson, G. N. Phillips Jr., *Chem. Rev.* **1994**, *94*, 699.
- [4] L. Pauling, *Nature* **1964**, *203*, 182.
- [5] S. E. V. Phillips, B. P. Schoenborn, *Nature* **1981**, *292*, 81.
- [6] B. Shaanan, *Nature* **1982**, *296*, 683; B. Shaanan, *J. Mol. Biol.* **1983**, *171*, 31.
- [7] T. Yonetani, H. Yamamoto, T. Iizuka, *J. Biol. Chem.* **1974**, *249*, 2168; M. Ikeda-Saito, M. Brunori, T. Yonetani, *Biochim. Biophys. Acta* **1978**, *533*, 173; T. Kitagawa, M. R. Ondrias, D. L. Rousseau, M. Ikeda-Saito, T. Yonetani, *Nature* **1982**, *298*, 869.
- [8] M. Matsu-ura, F. Tani, S. Nakayama, N. Nakamura, Y. Naruta, *Angew. Chem.* **2000**, *112*, 2083; *Angew. Chem., Int. Ed.* **2000**, *39*, 1989; F. Tani, M. Matsu-ura, S. Nakayama, M. Ichimura, N. Nakamura, Y. Naruta, *J. Am. Chem. Soc.* **2001**, *123*, 1133.
- [9] B. A. Springer, K. D. Egeberg, S. G. Sligar, R. J. Rohlfis, A. J. Mathews, J. S. Olson, *J. Biol. Chem.* **1989**, *264*, 3057.
- [10] J. S. Olson, G. N. Phillips Jr., *J. Biol. Chem.* **1997**, *2*, 544; W. D. Tian, J. T. Sage, P. M. Champion, *J. Mol. Biol.* **1993**, *233*, 155.
- [11] E. Antonini, M. Brunori, in 'Frontiers of Biology', Vol. 21, Eds. A. Neuberger, E. L. Tatum, North-Holland, Amsterdam, 1971.
- [12] G. Metz, T. Sjöstrand, *Acta Physiol. Scand.* **1954**, *31*, 384; R. F. Coburn, *Ann. N. Y. Acad. Sci.* **1970**, *174*, 11.

- [13] a) J. P. Collman, L. Fu, *Acc. Chem. Res.* **1999**, *32*, 455; b) M. Momenteau, C. A. Reed, *Chem. Rev.* **1994**, *94*, 659; c) T. G. Traylor, *Acc. Chem. Res.* **1981**, *14*, 102; d) R. D. Jones, D. A. Summerville, F. Basolo, *Chem. Rev.* **1979**, *79*, 139.
- [14] a) J. P. Collman, J. I. Brauman, B. L. Iverson, J. L. Sessler, R. M. Morris, Q. H. Gibson, *J. Am. Chem. Soc.* **1983**, *105*, 3052; b) D. Lavalette, C. Tétreau, J. Mispelter, M. Momenteau, J.-M. Lhoste, *Eur. J. Biochem.* **1984**, *145*, 555; c) T. G. Traylor, N. Koga, L. A. Deardurff, P. N. Swepston, J. A. Ibers, *J. Am. Chem. Soc.* **1984**, *106*, 5132; d) T. G. Traylor, S. Tsuchiya, D. Campbell, M. Mitchell, D. Stynes, N. Koga, *J. Am. Chem. Soc.* **1985**, *107*, 604; e) T. G. Traylor, N. Koga, L. A. Deardurff, *J. Am. Chem. Soc.* **1985**, *107*, 6504.
- [15] J. P. Collman, R. R. Gagne, C. A. Reed, W. T. Robinson, G. A. Rodley, *Proc. Natl. Acad. Sci. U.S.A.* **1974**, *71*, 1326; G. B. Jameson, G. A. Rodley, W. T. Robinson, R. R. Gagne, C. A. Reed, J. P. Collman, *Inorg. Chem.* **1978**, *17*, 850.
- [16] a) J. P. Collman, R. R. Gagne, T. R. Halbert, J.-C. Marchon, C. A. Reed, *J. Am. Chem. Soc.* **1973**, *95*, 7868; b) J. P. Collman, R. R. Gagne, C. A. Reed, T. R. Halbert, G. Lang, W. T. Robinson, *J. Am. Chem. Soc.* **1975**, *97*, 1427.
- [17] G. B. Jameson, R. S. Drago, *J. Am. Chem. Soc.* **1985**, *107*, 3017.
- [18] J. P. Collman, J. I. Brauman, T. R. Halbert, K. S. Suslick, *Proc. Natl. Acad. Sci. U.S.A.* **1976**, *73*, 3333.
- [19] E. J. Heidner, R. C. Ladner, M. F. Perutz, *J. Mol. Biol.* **1976**, *104*, 707; T.-Y. Teng, V. Srajer, K. Moffat, *Nat. Struct. Biol.* **1994**, *1*, 701; M. L. Quillin, R. M. Arduini, J. S. Olson, G. N. Phillips Jr., *J. Mol. Biol.* **1993**, *234*, 140; I. Schlichting, J. Berendzen, G. N. Phillips Jr., R. M. Sweet, *Nature* **1994**, *371*, 808; D. Ivanov, J. T. Sage, M. Keim, J. R. Powell, S. A. Asher, P. M. Champion, *J. Am. Chem. Soc.* **1994**, *116*, 4139; Z. Derewenda, G. Dodson, P. Emsley, D. Harris, K. Nagai, M. Perutz, J.-P. Reynaud, *J. Mol. Biol.* **1990**, *211*, 515; E. A. Padlan, W. E. Love, *J. Biol. Chem.* **1974**, *249*, 4067; J. C. Norvell, A. C. Nunes, B. P. Schoenborn, *Science* **1975**, *190*, 568; J. P. Collman, J. I. Brauman, K. M. Doxsee, *Proc. Natl. Acad. Sci. USA* **1979**, *76*, 6035.
- [20] T. Li, M. L. Quillin, G. N. Phillips Jr., J. S. Olson, *Biochemistry* **1994**, *33*, 1433; J. Ling, T. Li, J. S. Olson, D. F. Bocian, *Biochim. Biophys. Acta* **1994**, *1188*, 417.
- [21] H. Imai, S. Sekizawa, E. Kyuno, *Inorg. Chim. Acta* **1986**, *125*, 151; M. Momenteau, B. Looock, D. Lavalette, C. Tétreau, J. Mispelter, *J. Chem. Soc., Chem. Commun.* **1983**, 962; M. Momenteau, J. Mispelter, B. Looock, J.-M. Lhoste, *J. Chem. Soc., Perkin Trans. 1*, **1985**, 221.
- [22] a) J. P. Collman, X. Zhang, K. Wong, J. I. Brauman, *J. Am. Chem. Soc.* **1994**, *116*, 6245; b) J. P. Collman, P. C. Herrmann, L. Fu, T. A. Eberspacher, M. Eubanks, B. Boitrel, P. Hayoz, X. Zhang, J. I. Brauman, V. W. Day, *J. Am. Chem. Soc.* **1997**, *119*, 3481.
- [23] T. G. Spiro, *Science* **1995**, *270*, 221; M. Lim, T. A. Jackson, P. A. Anfinrud, *Science* **1995**, *269*, 962; G. B. Ray, X.-Y. Li, J. A. Ibers, J. L. Sessler, T. G. Spiro, *J. Am. Chem. Soc.* **1994**, *116*, 162; K. Chu, J. Vojtechovsky, B. H. McMahon, R. M. Sweet, J. Berendzen, I. Schlichting, *Nature* **2000**, *403*, 921; T. G. Spiro, P. M. Kozlowski, *Acc. Chem. Res.* **2001**, *34*, 137.
- [24] a) M. Momenteau, D. Lavalette, *J. Chem. Soc., Chem. Commun.* **1982**, 341; b) G. E. Wuenschell, C. Tétreau, D. Lavalette, C. A. Reed, *J. Am. Chem. Soc.* **1992**, *114*, 3346; c) C. K. Chang, B. Ward, R. Young, M. P. Kondylis, *J. Macromol. Sci., Pure Appl. Chem.* **1988**, *A25*, 1307; F. Tani, M. Matsu-ura, S. Nakayama, M. Ichimura, N. Kamakura, Y. Naruta, *J. Am. Chem. Soc.* **2001**, *123*, 1133.
- [25] K. Nagai, B. Luisi, D. Shih, G. Miyazaki, K. Imai, C. Poyart, A. De Young, L. Kwiatkowski, R. W. Noble, S.-H. Lin, N.-T. Yu, *Nature* **1987**, *329*, 858; J. S. Olson, A. J. Mathews, R. J. Rohlf, B. A. Springer, K. D. Egeberg, S. G. Sligar, J. Tame, J.-P. Renaud, K. Nagai, *Nature* **1988**, *336*, 265.
- [26] D. E. Goldberg, *Chem. Rev.* **1999**, *99*, 3371; D. M. Minning, A. J. Gow, J. Bonaventura, R. Braun, M. Dewhirst, D. E. Goldberg, J. S. Stamler, *Nature* **1999**, *401*, 497.
- [27] K. S. Suslick, M. M. Fox, *J. Am. Chem. Soc.* **1983**, *105*, 3507.
- [28] J. P. Collman, C. A. Reed, *J. Am. Chem. Soc.* **1973**, *95*, 2048.
- [29] J. Geibel, J. Cannon, D. Campbell, T. G. Traylor, *J. Am. Chem. Soc.* **1978**, *100*, 3575; J. P. Collman, J. I. Brauman, K. M. Doxsee, T. R. Halbert, E. Bunnenberg, R. E. Linder, G. N. LaMar, J. Del Gaudio, G. Lang, K. Spartalian, *J. Am. Chem. Soc.* **1980**, *102*, 4182.
- [30] P. E. Ellis, J. E. Linard, T. Szymanski, R. D. Jones, J. R. Budge, F. Basolo, *J. Am. Chem. Soc.* **1980**, *102*, 1889.
- [31] J. P. Collman, J. I. Brauman, T. J. Collins, B. L. Iverson, G. Lang, R. B. L. Pettman, J. L. Sessler, M. A. Walter, *J. Am. Chem. Soc.* **1983**, *105*, 3038.
- [32] a) J. P. Collman, X. Zhang, K. Wong, J. I. Brauman, *J. Am. Chem. Soc.* **1994**, *116*, 6245; b) J. P. Collman, P. C. Herrmann, L. Fu, T. A. Eberspacher, M. Eubanks, B. Boitrel, P. Hayoz, X. Zhang, J. I. Brauman, V. W. Day, *J. Am. Chem. Soc.* **1997**, *119*, 3481.

- [33] G. R. Newkome, C. N. Moorefield, F. Vögtle, 'Dendritic Molecules: Concepts, Synthesis, Perspectives', VCH, Weinheim, 1996; M. Fischer, F. Vögtle, *Angew. Chem.* **1999**, *111*, 934; *Angew. Chem., Int. Ed.* **1999**, *38*, 884; O. A. Matthews, A. N. Shipway, J. F. Stoddart, *Prog. Polym. Sci.* **1998**, *23*, 1; C. B. Gorman, J. C. Smith, *Acc. Chem. Res.* **2001**, *34*, 60.
- [34] D.-L. Jiang, T. Aida, *Chem. Commun.* **1996**, 1523; D.-L. Jiang, T. Aida, *J. Macromol. Sci., Pure Appl. Chem.* **1997**, *A34*, 2047.
- [35] J. P. Collman, L. Fu, A. Zingg, F. Diederich, *Chem. Commun.* **1997**, 193.
- [36] P. Weyermann, F. Diederich, *J. Chem. Soc., Perkin Trans. 1* **2000**, 4231.
- [37] S. Hecht, J. M. J. Fréchet, *Angew. Chem.* **2001**, *113*, 76; *Angew. Chem., Int. Ed.* **2001**, *40*, 74; D. K. Smith, F. Diederich, *Top. Curr. Chem.* **2000**, *210*, 183; D. K. Smith, F. Diederich, *Chem. Eur. J.* **1998**, *4*, 1353.
- [38] D. A. Tomalia, A. M. Naylor, W. A. Goddard III, *Angew. Chem.* **1990**, *102*, 119; *Angew. Chem., Int. Ed.* **1990**, *29*, 138; G. R. Newkome, Z. Yao, G. R. Baker, V. K. Gupta, *J. Org. Chem.* **1985**, *50*, 2003; D. A. Tomalia, H. Baker, J. Dewald, M. Hall, G. Kallos, S. Marin, J. Roeck, J. Ryder, P. Smith, *Polym. J.* **1985**, *17*, 117.
- [39] a) P. J. Dandliker, F. Diederich, M. Gross, C. B. Knobler, A. Louati, E. M. Sanford, *Angew. Chem.* **1994**, *106*, 1821; *Angew. Chem., Int. Ed.* **1994**, *33*, 1739; b) P. J. Dandliker, F. Diederich, J.-P. Gisselbrecht, A. Louati, M. Gross, *Angew. Chem.* **1995**, *107*, 2906; *Angew. Chem., Int. Ed.* **1995**, *34*, 2725; c) P. J. Dandliker, F. Diederich, A. Zingg, J.-P. Gisselbrecht, M. Gross, A. Louati, E. Sanford, *Helv. Chim. Acta* **1997**, *80*, 1773.
- [40] C. Hawker, J. M. J. Fréchet, *J. Chem. Soc., Chem. Commun.* **1990**, 1010; T. M. Miller, T. X. Neenan, *Chem. Mater.* **1990**, *2*, 346; C. J. Hawker, J. M. J. Fréchet, *J. Am. Chem. Soc.* **1990**, *112*, 7638.
- [41] D. K. Smith, F. Diederich, *Chem. Commun.* **1998**, 2501; D. K. Smith, A. Zingg, F. Diederich, *Helv. Chim. Acta* **1999**, *82*, 1225.
- [42] T. Tsunoda, Y. Yamamiya, Y. Kawamura, S. Ito, *Tetrahedron Lett.* **1995**, *36*, 2529; O. Mitsunobu, *Synthesis* **1981**, *49*, 1.
- [43] N. J. Rose, R. S. Drago, *J. Am. Chem. Soc.* **1959**, *81*, 6138; T. J. Beugelsdijk, R. S. Drago, *J. Am. Chem. Soc.* **1975**, *97*, 6466.
- [44] R. MacQuarrie, Q. H. Gibson, *J. Biol. Chem.* **1971**, *246*, 5832; K. Imai, T. Yonetani, M. Ikeda-Saito, *J. Mol. Biol.* **1977**, *109*, 83; J. LaGow, L. J. Parkhurst, *Biochemistry* **1972**, *11*, 4520; M. H. Keyes, M. Falley, R. Lumry, *J. Am. Chem. Soc.* **1971**, *93*, 2035.
- [45] Q. H. Gibson, M. H. Smith, *Proc. Roy. Soc. London Ser. B* **1965**, *163*, 206; T. Okazaki, J. B. Wittenberg, *Biochim. Biophys. Acta* **1965**, *111*, 503; J. B. Wittenberg, C. A. Appleby, B. A. Wittenberg, *J. Biol. Chem.* **1972**, *247*, 527; A. P. Klock, J. Yang, F. S. Mathews, D. E. Goldberg, *J. Biol. Chem.* **1993**, *268*, 17669.
- [46] W. Linke, A. Seidell, 'Solubilities of Inorganic and Metallorganic Compounds', Van Nostrand, Princeton, 1958.
- [47] J. L. Hoard, *Science* **1971**, *174*, 1295; K. Spartalian, G. Lang, J. P. Collman, R. R. Gagne, C. A. Reed, *J. Chem. Phys.* **1975**, *63*, 5375.
- [48] F. A. Walker, M.-W. Lo, M. T. Ree, *J. Am. Chem. Soc.* **1976**, *98*, 5552; D. Brault, M. Rougee, *Biochemistry* **1974**, *13*, 4591; W. R. Scheidt, C. A. Reed, *Chem. Rev.* **1981**, *81*, 543.
- [49] S. De Backer, Y. Prinzie, W. Verheijen, M. Smet, K. Desmedt, W. Dehaen, F. C. De Schryver, *J. Phys. Chem. A* **1998**, *102*, 5451.
- [50] S. A. Vinogradov, L.-W. Lo, D. F. Wilson, *Chem. Eur. J.* **1999**, *5*, 1338.

Received July 3, 2001